Two- and three-particle complexes with logarithmic interaction: Compact wave functions for two-dimensional excitons and trions

J. C. del Valle [1,*] J. A. Segura Landa,[2] and D. J. Nader [3]

[1]*Institute of Mathematics, University of Gdańsk, ul. Wit Stwosz 57, 80-308 Gdańsk, Poland*

[2]*Facultad de Física, Universidad Veracruzana, Circuito Aguirre Beltrán s/n, Xalapa, Veracruz 91000, Mexico*

[3]*Department of Chemistry, Brown University, Providence, Rhode Island 02912, USA*

(Received 24 February 2023; accepted 25 September 2023; published 19 October 2023)

Assuming a logarithmic interaction between constituent particles, compact and locally accurate wave functions that describe bound states of the two-particle neutral, and three-particle charged complexes in two dimensions are designed. Prime examples of these complexes are excitons and trions that appear in monolayers of transition-metal dichalcogenides (TMDCs). In the case of excitons, these wave functions led to five to six correct decimal digits in the energy and the diamagnetic shifts. In addition, it is demonstrated that they can be used as zero-order approximations to study magnetoexcitons via perturbation theory in powers of the magnetic field strength. For the trion, making a comparison with experimental data for concrete TMDCs, we established that the logarithmic potential leads to binding energies $\lesssim 30\%$ greater than experimental ones. Finally, the structure of the wave function at small and large distances was established for excitons whose carriers interact via the Rytova-Keldysh potential.

DOI: 10.1103/PhysRevB.108.155421

I. INTRODUCTION

It was established long ago [1,2] that a logarithmic interaction between free electrons (e^-) and holes (h) may occur in two-dimensional semiconductors as a limiting case of the Rytova-Keldysh potential.[1] Let us consider a thin film/layer with a dielectric surrounding made of dielectric substrates. If the thickness is sufficiently small compared with the exciton Bohr radius, a logarithmic interaction between carriers confined to the film emerges as a result of the polarization of atomic orbitals [3]. Monolayers of transition-metal dichalcogenides (TMDCs) are relevant examples of this kind of film-substrate configurations. Such monolayers can be considered as two dimensional since their thickness is a few Angstroms [4]. The low dimensionality (planar) and dielectric screening in such materials result in a strong electrostatic interaction. It allows the existence of stable bound states for complexes composed by electrons and holes, such as excitons (e^-, h), and positively and negatively charged trions: (e^-, h, h) and (e^-, e^-, h), respectively. Monolayers of TMDCs have recently received special attention for being ideal candidates for potential applications in optoelectronics [5,6], valleytronics [7], enhanced photoluminescence [8,9], and systems with pronounced many-body effects [5]. In particular, the optical response of these materials is explained in terms of complexes [3]. For a multilayer configuration of TMDCs, the pair-wise interaction between two carriers of charge q_i and q_j within the same layer remains logarithmic,[2] having the same form as for monolayers:

$$V_{ij}(\rho) = -\frac{q_i q_j}{\rho_0} \ln\left(\frac{\rho}{\rho_0}\right). \tag{1}$$

Here, ρ denotes the relative distance between the carriers, whose electric charges are q_i and q_j, and

$$\rho_0 = \frac{d\,(\varepsilon_{||} - 1)}{2}, \tag{2}$$

where $\varepsilon_{||}$ is the in-plane component of the dielectric permittivity tensor of the bulk layered material, and d is the distance between layers.

In the effective-mass approximation, the quantum mechanical description of complexes is governed by the Schrödinger equation. In this context, the variational method has shown to be an adequate tool to study bound states of excitons and trions, see [11–16] and references therein. However, as mentioned in [17], difficulties in constructing a reasonable wave function ansatz in the case of larger complexes than excitons hinders the straightforward extension of the variational consideration. To overcome this drawback, some recent advances have been made in constructing adequate wave functions for intralayer trions [14,18]. However, most of the variational functions favor the simplicity in calculations leading to reasonable results in terms of energy, instead of a correct description of the wave function. The main goal of this work is to show that, for two/three-particle complexes, both accurate energies and wave functions can be simultaneously achieved by using adequate compact trial functions.

*Corresponding author: juan.delvalle@ug.edu.pl

[1]See Sec. IV for a detailed discussion based on excitons.

[2]For a detailed discussion and derivation of the interaction see [10], the Supplemental Material of [3].

In the present study, we construct compact ansätze (trial functions) associated with the intralayer exciton of multi and monolayers made of TMDCs using the internal structure of the exact wave functions in the logarithmic regime of interaction. For unclear reasons to the authors, this approach has not been studied so far in a variational consideration. We focus on the construction of locally accurate approximations of the wave functions. They are valuable not only for finding energies and expectation values with high accuracy, but also for shedding some light on physical properties of the exact wave functions. In fact, the search for compact wave functions describing few-particle charged systems is an active field of research [19]. For example, they are widely used in atomic physics due to their usefulness to compute efficiently scattering cross sections [20] and matrix elements of singular operators [21]. In quasi-two-dimensional materials, the slow convergence of CI (configuration interaction) functions [22–24] has motivated the search for simple yet accurate wave functions for the description of hole-electron interaction.

As we show, our approximate solutions (taken as zero order approximation) lead to a convergent perturbation series to the exact solution. Two concrete physically relevant examples of application are discussed: (i) magnetoexcitons in a weak field regime; and most importantly, (ii) the construction of three-particle wave functions.

The present work is organized as follows. In Sec. II, we discuss the construction of compact parameter-dependent exciton wave functions. Concrete variational calculations for the spectrum of the first low-lying states are presented. We investigate the accuracy of the energy estimates using the nonlinearization procedure [25] and an alternative variational trial function. Then, we study the effect of a weak uniform magnetic field to the energy spectrum using perturbation theory taking our compact functions as zero order approximation. In this line, we discuss the (re)summation of perturbation series using Padé approximants. In Sec. III, taking as a building block the trial function constructed for the exciton, we propose a trial function for the ground state of the trion. We study the binding energy of the complex for concrete TMDCs and compare it with experimental results. A simple formula for the trion energy is provided. In Sec. IV, we discuss extensions of our consideration to the Rytova-Keldysh potential. Finally, we summarized our results in Conclusions.

II. TWO-PARTICLE SYSTEM: EXCITONS

Consider the neutral system made of two charged particles (hole and electron) interacting through potential (1). After separating the motion of the center of mass and using polar coordinates, we arrive at the familiar two-dimensional radial Schrödinger equation for the relative motion,

$$-\frac{\hbar^2}{2\mu}\left(\partial_\rho^2\psi+\frac{1}{\rho}\partial_\rho\psi\right)+\left[\frac{\hbar^2 m^2}{2\,\mu\rho^2}+\frac{e^2}{\rho_0}\ln\left(\frac{\rho}{\rho_0}\right)\right]\psi=E\,\psi,\qquad \rho\in[0,\infty), \tag{3}$$

where μ is the reduced mass,[3] e denotes the charge of the hole, and $\hbar$ is the reduced Planck constant. Any energy and wave function can be labeled by (n_ρ, m), but for simplicity we drop such labels for now. The radial quantum number takes the values $n_\rho = 0, 1, \ldots$, meanwhile the magnetic quantum number $m = 0, \pm1, \ldots$. Using the transformation via the dimensionless coordinate

$$\rho \to \left(\frac{\hbar^2\rho_0}{\mu\, e^2}\right)^{-\frac{1}{2}}\rho, \tag{4}$$

we remove the explicit presence of the constants $\hbar$, μ, ρ_0, and e from the Schrödinger equation which is transformed into its dimensionless form:

$$-\frac{1}{2}\left(\partial_\rho^2\psi+\frac{1}{\rho}\partial_\rho\psi\right)+\left[\frac{m^2}{2\,\rho^2}+\ln(\rho)\right]\psi=\varepsilon\,\psi. \tag{5}$$

In this equation, ε plays the role of dimensionless energy, and it is related to E through

$$E=\frac{e^2}{\rho_0}\,\varepsilon-\frac{e^2}{2\rho_0}\ln\left(\frac{\mu\, e^2\rho_0}{\hbar^2}\right). \tag{6}$$

The second term in (6) only provides the reference point to measure energies, and it has no relevant role. From (6), it is clear that the energy difference between two arbitrary states does not depend on the reduced mass μ. Since we are interested in bound states, we impose boundary conditions on (5) such that the normalizability requirement

$$\int_0^\infty |\psi(\rho)|^2\rho\, d\rho \;<\; \infty \tag{7}$$

is fulfilled. Under these considerations, Eq. (5) does not admit an exact solution: Energies and wave functions can only be found in approximate form. Interestingly, the same spectral problem defined by Eq. (5) can appear in another context. Indeed, the effect of a wiggly cosmic string for both massless and massive particle propagation along the string axis is governed by (5), see [26].

A. Ground state

Relevant information concerning the structure of the wave function can be revealed using asymptotic analysis. It is convenient to adopt the exponential representation of the wave function, namely

$$\psi_{n_\rho,m}(\rho)=\rho^{|m|}P_{n_\rho,m}(\rho^2)\exp(-\Phi_{n_\rho,m}(\rho))\,. \tag{8}$$

The unknown function $\Phi_{n_\rho,m}(\rho)$ is called phase, while P_{n_ρ} is a polynomial of degree n_ρ. Explicitly,

$$P_{n_\rho}(\rho^2)=\prod_{i=1}^{n_\rho}\left(\rho^2-\rho_i^2\right),\qquad P_0(\rho)\;\equiv\;1. \tag{9}$$

For a given state, this polynomial is determined by the position of the nodes ρ_i, $i=1,\ldots,n_\rho$. Thus, representation (8) is unambiguous [25]. The asymptotic series of the ground state

[3] By definition $\mu=\frac{m_e m_h}{m_e+m_h}$, where m_e and m_h are the electron and hole effective masses, respectively.

phase, $\Phi_{0,0}(\rho)$, shares properties with those for excited states. Hence, we focus on the quantum numbers $(n_\rho = 0, m = 0)$ from now on. In this case, (8) takes the form

$$\psi_{0,0}(\rho) = \exp(-\Phi_{0,0}(\rho)). \tag{10}$$

We construct the asymptotic series around two relevant points of the domain: $\rho = 0$ and $\rho = \infty$; small and large relative distances, respectively. At $\rho = 0$, it can be demonstrated that the asymptotic series of the phase has the following structure

$$\Phi_{0,0}(\rho) = \sum_{i=1}^{\infty} \sum_{j=0}^{i} a_{ij} \rho^{2i} \ln^j(\rho), \quad \rho \to 0, \tag{11}$$

where a_{ij} are coefficients with dependence on ε. As a consequence, the wave function has a similar asymptotic series,

$$\psi_{0,0}(\rho) = \sum_{i=0}^{\infty} \sum_{j=0}^{i} b_{ij} \rho^{2i} \ln^j(\rho), \quad \rho \to 0, \tag{12}$$

where b_{ij} are ε-dependent coefficients. On the other hand, the first terms of the asymptotic series of the phase at $\rho = \infty$ are

$$\Phi_{0,0}(\rho) = \rho\left[\sqrt{2\ln\rho} + \frac{1-\varepsilon}{\sqrt{2\ln\rho}} + \mathcal{O}((\ln\rho)^{-3/2})\right] + \frac{1}{2}\ln\rho + \cdots, \quad \rho \to \infty. \tag{13}$$

Note that the dominant term, $\mathcal{O}(\rho\sqrt{\ln\rho})$, does not depend on the energy. Therefore, the same leading term is expected for any bound state. Contrary to the series at $\rho = 0$, see (11), we were unable to find the general structure of the phase at $\rho = \infty$. However, for the particular purpose of this work, this piece of information is not required. At $\rho \to 0$, the phase of any state has the same structure of series (11). On the other hand, the wave function of any state has the following asymptotic expansion,

$$\psi_{n_\rho,m}(\rho) = \rho^{|m|} \sum_{i=0}^{\infty} \sum_{j=0}^{i} b_{ij} \rho^{2i} \ln^j(\rho), \quad \rho \to 0, \tag{14}$$

with coefficients b_{ij} depending on $\varepsilon_{n_\rho,m}$, and $|m|$. Using series (14), the real solutions of the equation $\psi_{n_\rho,m}(L) = 0$, with $L>0$ sufficiently large, define low-accuracy approximations to the low-lying energies and wave functions.

B. Compact trial function

Based on series (11), (12), and (13), we constructed a parameter-dependent approximation for the wave function of an arbitrary state (n_ρ, m). We followed the prescription described in [27], where it was applied successfully to the quartic anharmonic oscillator. Such prescription establishes the following: The approximate phase is the result of matching the series (11) and (13) in a minimal way, reproducing as many dominant growing terms in (13) as possible. This procedure is almost unambiguous and it leads to

$$\Phi^{(\text{approx})}_{n_\rho,m}(\rho) = \frac{A + (1-2B)\,\rho^2 \ln\rho + (C + B\rho^2)\ln(1 + D\rho^2)}{\sqrt{F^2\,(1 + D\rho^2) + \frac{1}{2}\rho^2 \ln\rho}} - \frac{A}{F}, \tag{15}$$

where $\{A, B, C, D, F\}$ are five (n_ρ, m)-dependent dimensionless parameters. By construction, the phase (15) reproduces functionally (same structure, but different coefficients) all the terms in the expansion at small distances (11), but only the leading one in the expansion at large distances (13). The approximate trial wave function of an arbitrary state (n_ρ, m) is given ultimately by

$$\psi^{(\text{approx})}_{n_\rho,m}(\rho) = \rho^{|m|} P_{n_\rho}(\rho^2) \times \exp\left(-\frac{A + (1-2B)\,\rho^2 \ln\rho + (C + B\rho^2)\ln(1 + D\rho^2)}{\sqrt{F^2\,(1 + D\rho^2) + \frac{1}{2}\rho^2 \ln\rho}} + \frac{A}{F}\right), \tag{16}$$

where the polynomial $P_{n_\rho}(\rho^2)$ is of the form (9), and it carries the information about the nodes. To fix the value of free parameters, we use the variational method imposing the orthogonalization constraints

$$\left\langle \psi^{(\text{approx})}_{n_\rho,m} \middle| \psi^{(\text{approx})}_{n'_\rho,m} \right\rangle = 0, \quad n'_\rho = 0, 1, \ldots, n_\rho. \tag{17}$$

These constraints define the position of the nodes. Thus, after fixing m, we move sequentially from the ground state (n_ρ=0) to a higher excited state $n_\rho > 0$. Under these constraints, we calculate the parameter-dependent expectation value of the Hamiltonian associated with (5), usually called variational energy and denoted by $\varepsilon^{(var)}_{n_\rho,m}$. Then, using an optimization procedure, we can find the configuration of parameters that minimize the variational energy. Only for states with quantum numbers $(n_\rho = 0, m)$, the variational principle guarantees that the variational energy is an upperbound of the exact energy. To ensure the square integrability of (16), the constraint $D > 0$ is imposed.

Concrete numerical calculations were carried out for the first low-lying states with $n_\rho \leqslant 6$ and $|m| \leqslant 4$. As a result, the variational energy was found with relative accuracy $\sim 10^{-6}$ or less. In Table I, we present the optimal parameters and the variational energies for the first seven S states. Meanwhile, nodes are obtained with five exact significant digits. It was confirmed by using the nonlinearization procedure and making alternative accurate variational calculations, see below. The optimized variational energies reach and sometimes overcome the best results found in the literature [3,28–30].

By construction, our wave functions $\psi^{(\text{approx})}_{n_\rho,m}$ are locally accurate, mainly due to the correct asymptotic behavior of the wave function at small and large distances. To check this, we can estimate the local accuracy of $\psi^{(\text{approx})}_{n_\rho,m}(\rho)$ using the nonlinearization procedure, via the perturbation

TABLE I. Dimensionless optimal parameters and variational energies $\varepsilon^{(var)}_{n_\rho,0}$ of the first six S states. Diamagnetic shifts are also presented. Displayed numbers are rounded.

n_ρ	A	B	C	D	F	$\varepsilon^{(var)}_{n_\rho,0}$	$\frac{1}{8}\langle\rho^2\rangle$
0	−0.2259	0.7684	0.1879	1.9102	0.9561	0.179 935	0.1363
1	−2.1430	0.9613	−0.0655	0.7327	1.5413	1.314 677	1.0363
2	−3.5415	1.0256	−0.3938	0.6052	1.8695	1.830 608	2.8459
3	−4.6212	1.0659	−0.6910	0.5576	2.1177	2.168 874	5.5630
4	−5.4135	1.0935	−0.9265	0.5393	2.3216	2.421 054	9.1873
5	−6.1751	1.1193	−1.1668	0.5214	2.4880	2.622 221	13.7150
6	−6.9278	1.1438	−1.4163	0.5044	2.6286	2.789 590	19.1070

series [25]

$$\psi^{(\text{exact})}_{n_\rho,m} = \psi^{(\text{approx})}_{n_\rho,m}(1-\phi_1-\phi_2\ldots). \tag{18}$$

Furthermore, the nonlinearization procedure dictates that

$$\varepsilon^{\text{exact}}_{n_\rho,m} = \varepsilon^{(var)}_{n_\rho,m} + \varepsilon_2 + \varepsilon_3 + \cdots, \tag{19}$$

if $\psi^{(\text{approx})}_{n_\rho,m}$ is chosen according to the above mentioned prescription. Numerical calculations for S sates established that corrections ϕ_n in (18) decrease as n grows, specifically $|\phi_{n+1}/\phi_n| \lesssim 10^{-1}$ for all ρ. Therefore, the local accuracy of wave functions is guaranteed. In turn, $|\varepsilon_{n+1}/\varepsilon_n| \lesssim 10^{-2}$, which indicates a fast rate of convergence of (19). In particular, the value of ε_2 suggests that our variational calculations lead to energies with 5–6 exact decimal digits. For the states considered, corrections in (18) and (19) were calculated using the Mathematica codes described in [31]. In Table II, we present explicit values of the first 11 corrections ε_n in (19) for the ground state (0,0). For this state, it is enough to consider the first three terms in (19) to reach the accuracy provided by the finite-element calculations, see [32].

C. Alternative trial function

The orthogonalization procedure used to determine the position of the nodes is accurate but impractical for highly excited states. For a given m, the n_ρ excited state requires $n_\rho - 1$ constraints in order to fulfill (17). To overcome this drawback, an alternative and efficient procedure is discussed in this section. This approach only requires the knowledge of the ground state functions $(0, m)$. Using the wave functions $\psi^{(\text{approx})}_{0,m}(\rho)$ with optimal parameters, we construct the expansion

$$\psi_{n_\rho,m}(\rho) \approx \psi^{(\text{approx})}_{0,m}(\rho) \times \sum_{i=0}^{N}\sum_{j=0}^{i} c^{(n_\rho,m)}_{i,j}\,\rho^{2i}\,\ln^j(\rho) \tag{20}$$

to describe any state. The factor $\psi^{(\text{approx})}_{0,m}$ guarantees the correct asymptotic dominant behavior at large ρ in our trial function (20). Based on the series at small ρ, an additional factor is introduced in the form of a partial sum of (12) in order to improve the small-ρ behavior. In this representation, any wave function (20) contains $(N+1)(N+2)/2$ terms. Using the linear variational principle, it is known that the energies and coefficients $c^{(m)}_{i,j}$ are determined by the secular equations (Rayleigh-Ritz method). Thus, this alternative procedure is a two-step variational consideration. To solve the secular equations, we use the Löwdin orthogonalization procedure [33] since the set of functions $\{\rho^{2i}\ln^j\rho\}$ is not orthogonal. In Table III, we present the energies of the low-lying states with quantum numbers $n_\rho \leqslant 4$ and $|m| \leqslant 5$ using $N = 12$. For all states considered, numerical results indicate that the rate of convergence is about 3–4 correct digits with an increment of N to $N+1$. In fact, using $N = 12$, we established 24 exact decimal digits for energies of all states considered. Comparing with our variational results, we established that our locally accurate approximations (16) lead to energies with 5–6 exact decimal digits, which is in agreement with our calculations via the nonlinearization procedure.

TABLE II. Logarithmic potential, the ground state (0,0): First ten sums of energy corrections. Digits in bold are invariant with respect to the next order correction. The value of $\varepsilon_{\text{exact}}$ was calculated with the function (20).

Approximation	Value	Correction	Value
$\varepsilon_0+\varepsilon_1$	**0.179 935 4**52 016 501 408 229 152	$-\varepsilon_2$	$5.1787914339321731\times10^{-8}$
$\varepsilon_0+\varepsilon_1+\varepsilon_2$	**0.179 935 400** 228 587 068 907 420	ε_3	$9.8170705093752\times10^{-11}$
$\varepsilon_0+\ldots+\varepsilon_3$	**0.179 935 400 32**6 757 774 001 172	$-\varepsilon_4$	$8.61541999679\times10^{-13}$
$\varepsilon_0+\ldots+\varepsilon_4$	**0.179 935 400 325** 896 232 001 493	ε_5	$9.200491318\times10^{-15}$
$\varepsilon_0+\ldots+\varepsilon_5$	**0.179 935 400 325 905** 432 492 811	$-\varepsilon_6$	1.16392216×10^{-16}
$\varepsilon_0+\ldots+\varepsilon_6$	**0.179 935 400 325 905 31**6 100 595	ε_7	1.681331×10^{-18}
$\varepsilon_0+\ldots+\varepsilon_7$	**0.179 935 400 325 905 317 7**81 927	$-\varepsilon_8$	2.7053×10^{-20}
$\varepsilon_0+\ldots+\varepsilon_8$	**0.179 935 400 325 905 317 75**4 874	ε_9	4.76×10^{-22}
$\varepsilon_0+\ldots+\varepsilon_9$	**0.179 935 400 325 905 317 755 3**50	$-\varepsilon_{10}$	9.0×10^{-24}
$\varepsilon_0+\ldots+\varepsilon_{10}$	**0.179 935 400 325 905 317 755 341**	ε_{11}	1.8×10^{-25}
$\varepsilon_{\text{exact}}$	0.179 935 400 325 905 317 755 341		

TABLE III. Energies (ε) of the first low-lying states with quantum numbers $n_\rho \leqslant 4$ and $|m| \leqslant 5$, see (6). Results were obtained with $N = 12$, see (20). Underlined digits correspond to those digits reproduced by the variational energies. All printed digits are exact: Confirmed with $N = 13$.

$n_\rho/\lvert m\rvert$	0	1
0	0.179 935 400 325 905 317 755 341	1.039 612 607 367 968 583 608 037
1	1.314 677 846 047 317 635 438 844	1.662 901 190 508 306 406 113 371
2	1.830 608 839 744 414 785 298 073	2.047 765 063 110 404 237 580 088
3	2.168 874 146 054 584 411 366 434	2.326 094 048 304 208 876 062 166
4	2.421 054 965 033 637 757 825 116	2.544 033 274 577 971 448 108 208
$n_\rho/\lvert m\rvert$	2	3
0	1.497 798 460 867 032 070 612 310	1.811 273 253 112 008 598 564 854
1	1.929 287 879 273 176 751 640 227	2.141 542 186 466 426 635 213 589
2	2.233 478 680 963 778 182 582 480	2.392 481 446 049 754 044 603 719
3	2.467 896 772 583 752 523 081 303	2.594 392 795 360 084 586 946 462
4	2.658 389 492 811 470 794 957 093	2.763 108 473 682 027 259 596 914
$n_\rho/\lvert m\rvert$	4	5
0	2.049 706 164 599 668 581 995 749	2.242 142 115 820 400 875 545 543
1	2.317 307 924 417 713 851 799 756	2.467 097 474 123 876 210 404 164
2	2.530 696 526 629 787 083 928 815	2.652 645 890 317 996 675 838 214
3	2.707 805 246 985 471 371 167 548	2.810 282 701 535 865 116 991 903
4	2.859 009 046 649 596 541 890 608	2.947 167 432 155 959 952 276 143

D. Magnetoexcitons: *s* states

Consider an exciton subjected to a time-independent magnetic field $\boldsymbol{B} = B\hat{\boldsymbol{z}}$.[4] As long as the momentum of the center of mass is zero, it can be shown [34–36] that the Schrödinger equation[5] for the relative motion describing S states is

$$-\frac{1}{2}\left(\partial_\rho^2\psi + \frac{1}{\rho}\partial_\rho\psi\right) + \left[\ln(\rho) + \frac{\gamma^2}{8}\rho^2\right]\psi = \varepsilon\,\psi, \quad (21)$$

where

$$\gamma = \frac{B}{B_0}, \quad B_0 = \frac{c\,e^3\,\mu^2}{\hbar^3}. \quad (22)$$

Equation (21) is written in variable (4). Note that B_0 is the exciton unit of magnetic field while ε is defined through (6). For weak magnetic fields, perturbation theory for $\varepsilon(\gamma)$ can be constructed in the form

$$\varepsilon(\gamma) = \varepsilon_0 + \sum_{n=1}^{\infty}\varepsilon_n\gamma^{2n}. \quad (23)$$

The first order correction (ε_1), given by

$$\varepsilon_1 = \tfrac{1}{8}\langle\rho^2\rangle \quad (24)$$

is called the diamagnetic shift. For S states, the experimental measurement of ε_1 reveals physical properties such as the exciton mass, size, and spin [37]. Taking our compact approximations, we calculated the diamagnetic shifts of the first S states with $0 \leqslant n_\rho \leqslant 6$ with an accuracy of five significant digits. Results are presented in Table I. To calculate higher order corrections $\varepsilon_{n>1}$, we used the nonlinearization procedure as described in [38]. There, it was applied to construct the strong coupling expansion of the cubic anharmonic oscillator, see Subsection A. In this way, we calculated higher corrections $\varepsilon_{n>1}$. Using as zero-order approximation (16), we established corrections with nine exact decimal digits. In Table IV, we present the first 11 corrections in (23) for the ground state. Following Dyson's argument, it is expected to be a divergent series. However, numerical results suggest that the second term in (23), namely

$$\Delta\varepsilon(\gamma) = \sum_{n=1}^{\infty}\varepsilon_n\gamma^{2n}, \quad (25)$$

is an alternating series and Padé resummable. For example, using a Padé approximant $P_5^6(\gamma^2)$ based on the first 11 corrections leads to accurate results in the domain $0 \leqslant \gamma \leqslant 1$ with four exact significant digits. In Fig. 1, we presented the plots of $\Delta\varepsilon(\gamma)$ for the first seven S states calculated through Padé approximants $P_5^6(\gamma^2)$.

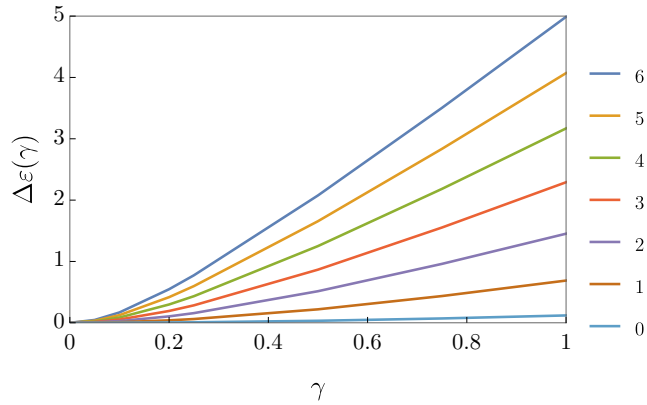

FIG. 1. Plot of $\Delta\varepsilon(\gamma)$ of magnetoexcitons with quantum numbers $0 \leqslant n_\rho \leqslant 6$ for $\gamma \in [0, 1]$. Plots constructed via Padé approximants $P_5^6(\gamma^2)$ of the perturbation series of each state.

[4]Therefore, the magnetic field is transversal to the thin film.

[5]In the symmetric gauge.

TABLE IV. Ground state (0,0): Numerical coefficients ε_n, $n = 0, 1, \ldots, 11$ of the series expansion (23) for ε calculated in nonlinearization procedure.

n	ε_n	n	ε_n
0	0.179 935 400	6	−0.018 000 868
1	0.136 337 679	7	0.030 034 032
2	−0.023 813 717	8	−0.057 913 120
3	0.0129 299 044	9	0.127 105 525
4	−0.011 145 815	10	−0.314 135 328
5	0.012 765 279	11	0.867 136 787

III. THREE-PARTICLE SYSTEM: TRIONS

In this section, we consider the lowest bound state of the two-dimensional complex made of three charged particles of (effective) masses (m_1, m_2, m_3) and charges $(-e, e, e)$, respectively. The pairwise interaction between them is assumed to be logarithmic, and it is given by (1). In Fig. 2, the geometrical setting of the system is shown.

The ground state is a square-integrable eigenfunction with dependence only on the relative distances $u_1 = r_{23}$, $u_2 = r_{13}$, and $u_3 = r_{12}$, and it is the lowest eigenfunction of the Hamiltonian[6]

$$\hat{H}_T \psi = E\psi, \quad \psi = \psi(u_1, u_2, u_3), \tag{26}$$

$$\hat{H}_T = -\frac{\hbar^2}{2}\Delta - \frac{e^2}{\rho_0}\ln\left(\frac{u_1}{\rho_0}\right) + \frac{e^2}{\rho_0}\ln\left(\frac{u_2}{\rho_0}\right) + \frac{e^2}{\rho_0}\ln\left(\frac{u_3}{\rho_0}\right), \tag{27}$$

with [40]

$$\begin{aligned}\Delta =& \frac{1}{\mu_{23}}\frac{1}{u_1}\partial_{u_1}(u_1\partial_{u_1}) + \frac{1}{\mu_{13}}\frac{1}{u_2}\partial_{u_2}(u_2\partial_{u_2}) \\ &+ \frac{1}{\mu_{12}}\frac{1}{u_3}\partial_{u_3}(u_3\partial_{u_3}) + \frac{1}{m_1}\frac{u_2^2+u_3^2-u_1^2}{u_2u_3}\partial_{u_3}\partial_{u_2} \\ &+ \frac{1}{m_2}\frac{u_1^2+u_3^2-u_2^2}{u_1u_3}\partial_{u_1}\partial_{u_3} + \frac{1}{m_3}\frac{u_1^2+u_2^2-u_3^2}{u_1u_2}\partial_{u_1}\partial_{u_2},\end{aligned} \tag{28}$$

[6]The ranges of the three variables u_i are coupled and satisfy a triangle condition: Their lengths must be such that they can form a triangle [39].

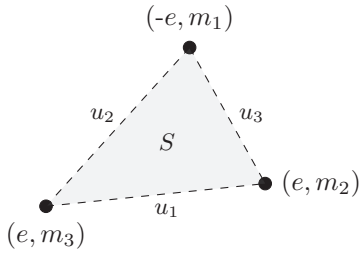

FIG. 2. Two-dimensional complex of three particles. Each constituent particle is labeled by (q, m), where q is the charge while m the mass. The area enclosed, denoted by S and shaded in gray, is given by (30).

where

$$\mu_{ij} = \frac{m_i m_j}{m_i + m_j}, \quad i, j = 1, 2, 3 \tag{29}$$

are the reduced masses. The operator $\hat{H}_T$ is self-adjoint with respect to the volume element

$$dV \propto u_1 u_2 u_3 S^{-1}\, du_1\, du_2\, du_3\,,$$
$$S = \tfrac{1}{4}\sqrt{(u_1+u_2+u_3)(u_1+u_2-u_3)(u_2+u_3-u_1)(u_1+u_3-u_2)}. \tag{30}$$

We set $m_2 = m_3$, as it usually appears in trions.[7] Under this assumption,

$$\mu_{12} = \mu_{13}, \quad \mu_{23} = \frac{m_{2,3}}{2}. \tag{31}$$

Next, we introduce the following change of variables

$$u_i \to \left(\frac{\hbar^2\rho_0}{m_1 e^2}\right)^{-\frac{1}{2}} u_i, \quad i = 1, 2, 3, \tag{32}$$

and the parameter

$$\sigma = \frac{m_1}{m_{2,3}} \tag{33}$$

to remove in (26) the appearance of physical constants (except for the masses m_1 and $m_2 = m_3$). Therefore, the trion ground state wave function corresponds to the nodeless solution of the dimensionless equation

$$-\frac{1}{2}\Delta_\sigma\psi + \ln\left(\frac{u_2u_3}{u_1}\right)\psi = \varepsilon(\sigma)\,\psi, \tag{34}$$

where

$$\begin{aligned}\Delta_\sigma =& \frac{2\sigma}{u_1}\partial_{u_1}(u_1\partial_{u_1}) + \frac{\sigma+1}{u_2}\partial_{u_2}(u_2\partial_{u_2}) + \frac{\sigma+1}{u_3}\partial_{u_3}(u_3\partial_{u_3}) \\ &+ \frac{u_2^2+u_3^2-u_1^2}{u_2u_3}\partial_{u_3}\partial_{u_2} + \sigma\frac{u_1^2+u_3^2-u_2^2}{u_1u_3}\partial_{u_1}\partial_{u_3} \\ &+ \sigma\frac{u_1^2+u_2^2-u_3^2}{u_1u_2}\partial_{u_1}\partial_{u_2}.\end{aligned} \tag{35}$$

In (34), $\varepsilon(\sigma)$ is related to the total energy (E) as follows:

$$E = \frac{e^2}{\rho_0}\varepsilon(\sigma) - \frac{e^2}{2\rho_0}\ln\left(\frac{m_1e^2\rho_0}{\hbar^2}\right). \tag{36}$$

[7]It has been established that for monolayers of TMDCs based of Tungsten, electrons in negative trions may have different effective masses, see [41].

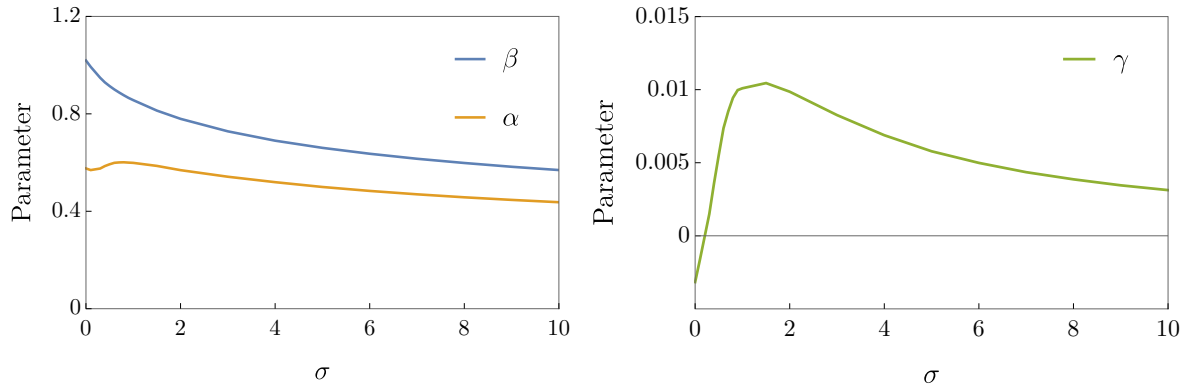

FIG. 3. Dimensionless optimal variational parameters of ansatz (37) as functions of the mass ratio σ.

In contrast to the energy levels of an exciton, the difference in energy of two arbitrary levels does depend on the masses through σ.

A. Trial function

Based on the functions (16) constructed for excitons in Sec. II, we design compact trial functions for a trion in its ground state. Since we assumed that $m_2 = m_3$, the positively charged trion (e^-, h, h) and the negative one (h, e^-, e^-) are described by the same Schrödinger equation.[8] Their total wave functions, which include spin and valley quantum numbers, are antisymmetric with respect to the permutation of identical particles, see [18]. In particular, the spatial part of the ground state wave function must be symmetric[9] under this permutation. Therefore, we propose the following symmetric wave function:

$$\psi^{(\mathrm{approx})}(u_1, u_2, u_3) = \hat{S}\big[\big(1 + \gamma\, u_1^2 \ln\big(u_1^2\big)\big)\, e^{-\Phi_{0,0}(\alpha^2 u_2) - \Phi_{0,0}(\beta^2 u_3)}\big], \tag{37}$$

where the symmetrizer operator is given by

$$\hat{S} = \tfrac{1}{2}(1 + \hat{P}_{23}). \tag{38}$$

Here $\hat{P}_{23}$ is the permutation between the identical particles $2 \to 3$ in u variables. The form of the phase is given in (15). Note that $\Phi_{0,0}$ is given by formula (15) with optimized parameters found in Table I. The construction of the previous wave function is motivated as follows. The factor $e^{-\Phi_{0,0}(\alpha^2 u_2) - \Phi_{0,0}(\beta^2 u_3)}$ describes the trion when the repulsive term of the interaction is absent. In turn, the factor $1 + \gamma u_1^2 \ln(u_1^2)$ takes into account the polarization of the complex and describes the repulsion between equally charged carriers. This fact can be easily established using asymptotic analysis in (34) at small u_1, which leads to the expansion

$$\psi(u_1, u_2, u_3) = 1 - \frac{1}{4\sigma}\, u_1^2 \ln(u_1) + \frac{1}{2(\sigma+1)}(u_2^2 \ln(u_2) + u_1^2 \ln(u_3)) + \cdots. \tag{39}$$

Parameters $\{\alpha, \beta\}$ were introduced in such a way that (i) they admit the meaning of screening charges if m_1 is kept fixed; and (ii) the square integrability of the trial function is guaranteed. Altogether, the trial function (37) contains only three free real parameters: $\{\alpha, \beta, \gamma\}$. To fix their values, we use the variational method to find the optimal configuration that minimizes the variational energy. Numerical calculations were performed in perimetric coordinates using a modification of the FORTRAN code described in [43].

We carried out calculations for $\sigma \in [0, 10]$, thus, covering representative TMDCs (see below). In Fig. 3, we present the optimal parameters as functions of σ in the domain $\sigma \in [0, 10]$. They have a smooth behavior, especially at large σ. We found that $\beta > \alpha$ in the domain considered. It hints that one of the two equally charged carriers is closer to the opposite-charged one. Compared to α and β, parameter γ is smaller. It reaches its maximum value at $\sigma \sim 1 - 2$. In Table V, optimized variational energy $\varepsilon(\sigma)$ is presented.

B. Alternative trial function

To investigate the accuracy of the variational calculations shown in the previous section, we use an alternative trial function to estimate the energy of the trion in the lowest S state with higher accuracy. In a similar way it was done for the exciton, see (20), we proposed

$$\psi(u_1, u_2, u_3) = \hat{S}\Bigg[\sum_{i,j,k=0}^{N} c_{i,j,k}\, u_1^{2i} u_2^{2j} u_3^{2k} \big(1 + \gamma\, u_1^2 \ln\big(u_1^2\big)\big) \times e^{-\Phi_{0,0}(\alpha^2 u_2) - \Phi_{0,0}(\beta^2 u_3)}\Bigg], \tag{40}$$

where $c_{i,j,k}$ are coefficients to be determined. Without loss of generality, we set $c_{0,0,0} = 1$ as normalization of the approximate wave function. Note that at $N = 0$, trial functions (37) and (40) coincide. Meanwhile at $N > 0$, they differ due to the insertion of the polynomial prefactor $\sim u_1^{2i} u_2^{2j} u_3^{2k}$. This insertion corrects the behavior of the wave function at small

[8] When the constituent particles have different masses, they are distinguishable. Consequently, no symmetry requirement is imposed to the total wave function. In particular, in (37) the symmetrizer is no longer needed.

[9] According to our variational calculations, the antisymmetric S state is repulsive and does not correspond to a bound state. This feature was already established for the Rytova-Keldysh potential in the nonlogarithmic regime, see [18,42].

TABLE V. Trion dimensionless energy $\varepsilon(\sigma)$ vs the mass ratio σ, see (36). Variational energies obtained through trial functions (37) and (40). For the latter, calculations correspond to $N = 1$, which were confirmed with $N = 2$. Results rounded to first display decimal digits.

	Wave function			Wave function	
σ	Eq. (37)	Eq. (40)	σ	Eq. (37)	Eq. (40)
0	0.0871	0.0791	1	0.42265	0.4182
0.1	0.1365	0.1285	2	0.6091	0.6058
0.2	0.1809	0.1729	3	0.7450	0.7411
0.3	0.2202	0.2165	4	0.8506	0.8473
0.4	0.2563	0.2539	5	0.9378	0.9347
0.5	0.2891	0.2868	6	1.0117	1.0090
0.6	0.3194	0.3166	7	1.0763	1.0737
0.7	0.3476	0.3443	8	1.1333	1.1308
0.8	0.3740	0.3703	9	1.1845	1.1821
0.9	0.3990	0.3949	10	1.2309	1.2286

distances, leading to a higher accuracy for the ground state energy. To fix the value of the parameters $\{\alpha, \beta, \gamma\}$ and $c_{i,j,k}$'s, we followed a two-step variational consideration. First, we fix the value of parameters $\{\alpha, \beta, \gamma\}$ according to the variational calculations of the previous section, in which the polynomial prefactor was not considered. The remaining free parameters, $c_{i,j,k}$'s, are defined by means of the secular equations. To solve them, we used the Löwdin orthogonalization procedure. In Table V, we present the value of $\varepsilon(\sigma)$ calculated with $N = 1$ in (40) for representative values of σ. Using $N = 2$, we confirmed the results for $N = 1$ up to the first four decimal digits. It indicates a fast rate of convergence with respect to N. In this way, we concluded that the wave function (37) provides an accuracy of two decimal digits for all $\sigma > 0$.

The plot of $\varepsilon(\sigma)$, calculated through trial function (40) with $N = 1$, is shown in Fig. 4. The curve described by $\varepsilon(\sigma)$ can be easily interpolated with an accuracy of two decimal digits by the simple function

$$\varepsilon_{fit}(\sigma) = a + b\,\ln(1 + c\,\sigma),$$
$$a = 0.083, \quad b = 0.465, \quad c = 1.059, \tag{41}$$

in the domain $\sigma \in [0, 10]$.

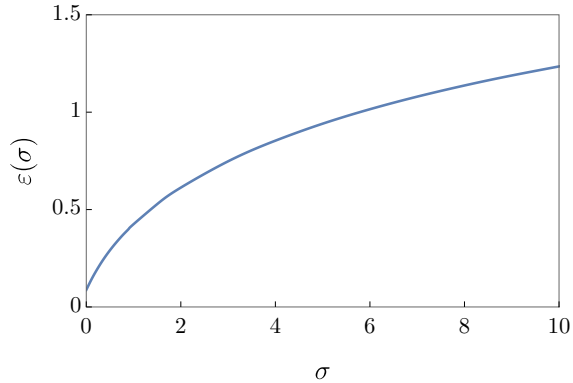

FIG. 4. Plot of dimensionless energy of trions ε, see (36), as a function of the mass ratio σ.

C. Comparison with experimental data

In order to compare our results with experimental data, we calculated the binding energy (E_b). It is defined as the amount of energy needed to dissociate a trion into a neutral complex (exciton) and a free carrier. Therefore,

$$E_b = |E_{\text{trion}} - E_{\text{exciton}}|, \tag{42}$$

where the energies correspond to ground states. According to (6), (36), and (41), we have a compact expression for E_b,

$$E_b(\sigma) = \frac{e^2}{\rho_0}\big[0.179935 - \varepsilon_{fit}(\sigma) + \tfrac{1}{2}\ln(1+\sigma)\big]. \tag{43}$$

Hence, the binding energy for trions is a function of σ.

In Table VI, we compare theoretical binding energies given by (43) with experimental ones for negatively charged trions[10] in molybdenum (Mo) and tungsten (W) dichalcogenide materials. As previously established [44], we found that logarithmic potential overbinds the trion, leading to larger binding energies than those reported in experiments. However, our results do not confirm the statement that the logarithmic potential leads to binding energies 50% larger, see [44]. The largest deviation occurs for $MoSe_2$, reaching a deviation in energies of 30%. In turn, the smallest deviation is found for WS_2, for which is 16%. Interestingly, either formula (43) or experimental results predicts equal binding energy for MoS_2 and WS_2.

IV. TOWARD THE RYTOVA-KELDYSH POTENTIAL

If ρ_0 in (1) is comparable to the exciton Bohr radius, the logarithmic potential (1) is no longer suitable to describe the interaction between carriers inside monolayers of TMDCs. Furthermore, it overbinds three-particle complexes as we have seen. Under these circumstances, an adequate description of the interaction is given by the celebrated Rytova-Keldysh potential [1,2], namely

$$V_{RK}(\rho) = \frac{\pi q_i q_j}{2\rho_0} W\left(\frac{\rho}{\rho_0}\right), \tag{44}$$

[10]Thus, we take $m_1 = m_h$ and $m_2 = m_e$.

TABLE VI. Negative charged trion binding energy in meV for different suspended TMDC monolayers. Results rounded to first displayed significant digits. Values of ρ_0, σ, and experimental binding energies taken from reference [45].

Material	ρ_0 (Å)	σ	E_b (meV)	
			Present results	Experiments
MoS_2	39	0.81	41	34, 35
$MoSe_2$	40	0.86	39	30
WS_2	38	0.84	41	34, 36
WSe_2	45	0.85	35	30

where

$$W\left(\frac{\rho}{\rho_0}\right) = H_0\left(\frac{\rho}{\rho_0}\right) - Y_0\left(\frac{\rho}{\rho_0}\right). \tag{45}$$

Here H_0 and Y_0 are the Struve and Bessel function of second kind, respectively. At small ρ, the Rytova-Keldysh potential is reduced to the logarithmic potential as follows:

$$V_{RK}(\rho) = -\frac{q_i q_j}{\rho_0}\left[\ln\left(\frac{\rho}{\rho_0}\right) + \Gamma - \frac{\rho}{\rho_0} + \mathcal{O}(\rho^2 \ln \rho)\right], \quad \rho \to 0, \tag{46}$$

where $\Gamma = \gamma - \ln 2$; here γ denotes the Euler-Mascheroni constant. The constant Γ fixes the reference point for the energy. Therefore, it plays no relevant physical role when studying binding energies of complexes interacting within the logarithmic regime. On the other hand, at large distances

$$V_{RK}(\rho) = \frac{q_i q_j}{\rho}\left[1 - \left(\frac{\rho_0}{\rho}\right)^2 + 9\left(\frac{\rho_0}{\rho}\right)^4 + \mathcal{O}(\rho^{-6})\right], \quad \rho \to \infty. \tag{47}$$

Therefore, in this limit, the dominant interaction is given by the Coulomb one. The radial Schrödinger equation that describes excitons now reads

$$-\frac{\hbar^2}{2\mu}\left(\partial_\rho^2\psi + \frac{1}{\rho}\partial_\rho\psi\right) + \left[\frac{\hbar^2 m^2}{2\mu\rho^2} - \frac{\pi e^2}{2\rho_0} W\left(\frac{\rho}{\rho_0}\right)\right]\psi = E\,\psi. \tag{48}$$

To construct a compact trial function for excitons, we can follow the approach presented in Sec. II B, in which the main ingredient is the asymptotic series. Using the transformation (4), we obtain the dimensionless Schrödinger equation

$$-\frac{1}{2}\left(\partial_\rho^2\psi + \frac{1}{\rho}\partial_\rho\psi\right) + \left[\frac{m^2}{2\rho^2} - \frac{\pi\lambda}{2} W(\lambda\rho)\right]\psi = \varepsilon\,\psi, \tag{49}$$

where[11]

$$\lambda = \frac{a_0}{\rho_0}, \quad \varepsilon = \frac{E}{\mathcal{E}_0}, \quad \mathcal{E}_0 = \frac{\mu e^4}{\hbar^2}. \tag{50}$$

Note that λ corresponds to the ratio of the two length scales of the system. According to parameters found in [45], $\lambda \lesssim 8\times10^{-2}$ for all materials presented in Table VI. Therefore, it suggests taking the potential in Eq. (49) and expanding it in powers of λ,

$$-\frac{\pi\lambda}{2} W(\lambda\rho) = \lambda\big[\ln(\lambda\rho) + \Gamma - \lambda\rho + \mathcal{O}(\lambda^2)\big], \quad \lambda \to 0. \tag{51}$$

Therefore, the logarithmic potential is dominant[12] at small λ. For arbitrary λ, an asymptotic analysis establishes that the phase of the exciton wave function has the asymptotic series

$$\Phi_{n_\rho,m}(\rho) = \sum_{i=1}^{\infty}\left\{\rho^{2i}\sum_{j=0}^{i} a_{ij}\ln^j(\rho) + \rho^{2i+1}\sum_{j=0}^{i-1} b_{ij}\ln^j(\rho)\right\}, \quad \rho \to 0, \tag{52}$$

where $a_{i,j}$ and b_{ij} are coefficients, cf. (11). Consequently, the wave function behaves as

$$\psi_{n_\rho,m}(\rho) = \rho^{|m|}\left(1 + \sum_{i=1}^{\infty}\left\{\rho^{2i}\sum_{j=0}^{i} A_{ij}\ln^j(\rho) + \rho^{2i+1}\sum_{j=0}^{i-1} B_{ij}\ln^j(\rho)\right\}\right), \quad \rho \to 0, \tag{53}$$

with A_{ij} and B_{ij} coefficients. At large distances, the phase acquires the following form:

$$\Phi_{n_r,m}(\rho) = \sqrt{-2\varepsilon}\,\rho + \frac{1}{2}(4n_\rho + 2m + 1)\ln\rho + \sum_{k=1}^{\infty} c_k \rho^{-k}, \tag{54}$$

where c_k's are coefficients. In contrast with (13), for the Keldysh-Rytova it is possible to find the structure exciton wave function at large distances. Certainly, it will lead to an improvement in terms of local accuracy of wave function and variational energies compared with the current trial functions based on hydrogenlike orbitals, see [11]. In our present approach, the next step to construct a compact wave function is the interpolation between series (53) and (54). A minimal interpolation results in

$$\Phi^{(\mathrm{approx})}_{n_\rho,m}(\rho) = \frac{A + B\rho^2\ln(1 + C\rho) + D\rho^3}{\sqrt{1 + F\rho^2\ln\rho + G\rho^4}} + \frac{1}{8}(4n_\rho + 2m + 1)\ln(1 + G\rho^4), \tag{55}$$

[11]Here a_0 denotes the exciton Bohr radius defined as $a_0 = \frac{\hbar^2}{\mu e^2}$. Meanwhile, $\mathcal{E}_0$ represents the exciton Rydberg constant.

[12]The same conclusion for the N-particle complex can be established using similar arguments.

where $\{A, B, C, D, F, G\}$ are free parameters. Once introduced in (8), it leads to the approximate form of the exciton wave function. Its accuracy in the framework of the variational method will be studied elsewhere. Finally, the three-particle compact wave functions can be constructed following the same procedure shown in this work: Going from two to three particles using the exciton wave function as a building block.

V. CONCLUSIONS

In this article, locally accurate wave functions were constructed for the bound states of two-particle system (exciton) in two dimensions whose constituent particles interact through a logarithmic potential. For states with quantum numbers $n_\rho \leqslant 4$ and $|m| \leqslant 5$, they allowed us to reproduce energies with 5–6 exact decimal digits. It was checked using the nonlinearization procedure and an alternative two-step variational approach. For magnetoexcitons at rest, it was demonstrated that those functions (used as a zero-order approximation) lead to highly accurate coefficients of the weak coupling energy expansion in powers of the magnetic field strength. Numerical results for S states suggest that the weak coupling expansion is Padé (re)summable.

We constructed a compact approximation of the two-dimensional three-particle system (trion) ground state wave function using the exciton ground state one as a building block. It only depends on three nonlinear free parameters that are fixed through the variational method. It contrasts with the 10^6 linear variational parameters that were recently used in [42]. Our wave function led to binding energies in good agreement with experimental results for trions in concrete TMDCs made of Mo, W, S, and Se. It was shown that the logarithmic potential leads to binding energies $\lesssim 30\%$ larger than those coming from experiments. We find a simple formula for the binding energy as a function of the mass ratio of the constituent particles.

Finally, the structure of the exciton wave function at small distances whose carriers interact via the Rytova-Keldysh potential was established. This new piece of information may lead to the construction of improved variational wave functions used to study larger complexes in TMDCs like biexcitons.

ACKNOWLEDGMENTS

The authors thank Prof. A. V. Turbiner for drawing our attention to logarithmic interactions as well as valuable comments and suggestions. We thank J. C. López-Vieyra for the support with the variational calculations. J. C. del Valle thanks D. A. Bonilla-Moreno for useful remarks and discussions. The authors thank M. Szyniszewski for his interest and for providing additional information on Ref. [45]. During the last stage of this work, J. C. del Valle was partially supported by the SONATA-BIS 9 Grant No. 2019/34/E/ST1/00390. D.J.N. acknowledges support by Fulbright COMEXUS Project No. P000003405.

[1] N. S. Rytova, The screened potential of a point charge in a thin film, Univ. Phys. Bull. **3**, 18 (1967).

[2] L. Keldysh, Coulomb interaction in thin semiconductor and semimetal films, J. Exp. Theor. Phys. **29**, 658 (1979).

[3] B. Ganchev, N. Drummond, I. Aleiner, and V. Fal'ko, Three-particle complexes in two-dimensional semiconductors, Phys. Rev. Lett. **114**, 107401 (2015), See Supplemental Material.

[4] H. Yang, A. Giri, S. Moon, S. Shin, J.-M. Myoung, and U. Jeong, Highly scalable synthesis of MoS_2 thin films with precise thickness control via polymer-assisted deposition, Chem. Mater. **29**, 5772 (2017).

[5] J. S. Ross, S. Wu, H. Yu, N. J. Ghimire, A. M. Jones, G. Aivazian, J. Yan, D. G. Mandrus, D. Xiao, W. Yao, and X. Xu, Electrical control of neutral and charged excitons in a monolayer semiconductor, Nat. Commun. **4**, 1474 (2013).

[6] Q. H. Wang, K. Kalantar-Zadeh, A. Kis, J. N. Coleman, and M. S. Strano, Electronics and optoelectronics of two-dimensional transition metal dichalcogenides, Nat. Nanotechnol. **7**, 699 (2012).

[7] Y. Liu, Y. Gao, S. Zhang, J. He, J. Yu, and Z. Liu, Valleytronics in transition metal dichalcogenides materials, Nano Res. **12**, 2695 (2019).

[8] A. Splendiani, L. Sun, Y. Zhang, T. Li, J. Kim, C.-Y. Chim, G. Galli, and F. Wang, Emerging photoluminescence in monolayer MoS2, Nano Lett. **10**, 1271 (2010).

[9] K. F. Mak, C. Lee, J. Hone, J. Shan, and T. F. Heinz, Atomically thin MoS_2: A new direct-gap semiconductor, Phys. Rev. Lett. **105**, 136805 (2010).

[10] V. M. Fomin and E. P. Pokatilov, Excitons in multi-layer systems, Phys. Status Solidi B **129**, 203 (1985).

[11] M. F. Martins Quintela and N. M. Peres, A colloquium on the variational method applied to excitons in 2D materials, Eur. Phys. J. B **93**, 1 (2020).

[12] F. Grasselli, Variational approach to the soft-Coulomb potential in low-dimensional quantum systems, Am. J. Phys. **85**, 834 (2017).

[13] J.-Z. Zhang and J.-Z. Ma, Two-dimensional excitons in monolayer transition metal dichalcogenides from radial equation and variational calculations, J. Phys.: Condens. Matter **31**, 105702 (2019).

[14] M. A. Semina, Excitons and trions in bilayer Van der Waals heterostructures, Phys. Solid State **61**, 2218 (2019).

[15] M. R. Molas, A. O. Slobodeniuk, K. Nogajewski, M. Bartos, L. Bala, A. Babiński, K. Watanabe, T. Taniguchi, C. Faugeras, and M. Potemski, Energy spectrum of two-dimensional excitons in a nonuniform dielectric medium, Phys. Rev. Lett. **123**, 136801 (2019).

[16] T. G. Pedersen, Exciton Stark shift and electroabsorption in monolayer transition-metal dichalcogenides, Phys. Rev. B **94**, 125424 (2016).

[17] I. Kylänpää and H.-P. Komsa, Binding energies of exciton complexes in transition metal dichalcogenide monolayers and effect of dielectric environment, Phys. Rev. B **92**, 205418 (2015).

[18] E. Courtade, M. Semina, M. Manca, M. M. Glazov, C. Robert, F. Cadiz, G. Wang, T. Taniguchi, K. Watanabe, M. Pierre, W. Escoffier, E. L. Ivchenko, P. Renucci, X. Marie, T. Amand, and

B. Urbaszek, Charged excitons in monolayer WSe_2: Experiment and theory, Phys. Rev. B **96**, 085302 (2017).

[19] D. Bressanini and G. Morosi, A compact boundary-condition-determined wavefunction for two-electron atomic systems, J. Phys. B **41**, 145001 (2008).

[20] M. Kircher, F. Trinter, S. Grundmann, G. Kastirke, M. Weller, I. Vela-Perez, A. Khan, C. Janke, M. Waitz, S. Zeller, T. Mletzko, D. Kirchner, V. Honkimäki, S. Houamer, O. Chuluunbaatar, Y. V. Popov, I. P. Volobuev, M. S. Schöffler, L. P. H. Schmidt, T. Jahnke *et al.*, Ion and electron momentum distributions from single and double ionization of helium induced by compton scattering, Phys. Rev. Lett. **128**, 053001 (2022).

[21] V. A. Yerokhin, V. Patkóš, and K. Pachucki, Atomic structure calculations of helium with correlated exponential functions, Symmetry **13**, 1246 (2021).

[22] J. Planelles, Simple correlated wave-functions for excitons in 0D, quasi-1D and quasi-2D quantum dots, Theor. Chem. Acc. **136**, 81 (2017).

[23] M. F. C. Martins Quintela and N. M. R. Peres, A colloquium on the variational method applied to excitons in 2D materials, Eur. Phys. J. B **93**, 222 (2020).

[24] J. Planelles and J. I. Climente, A simple variational quantum Monte Carlo-effective mass approach for excitons and trions in quantum dots, Comput. Phys. Commun. **261**, 107782 (2021).

[25] A. V. Turbiner, The eigenvalue spectrum in quantum mechanics and the nonlinearization procedure, Sov. Phys. Usp. **27**, 668 (1984).

[26] F. d. S. Azevedo, F. Moraes, F. Mireles, B. Berche, and S. Fumeron, Wiggly cosmic string as a waveguide for massless and massive fields, Phys. Rev. D **96**, 084047 (2017).

[27] A. V. Turbiner and J. C. del Valle, Anharmonic oscillator: A solution, J. Phys. A **54**, 295204 (2021).

[28] F. J. Asturias and S. R. Aragón, The hydrogenic atom and the periodic table of the elements in two spatial dimensions, Am. J. Phys. **53**, 893 (1985).

[29] K. Eveker, D. Grow, B. Jost, C. E. Monfort, III, K. W. Nelson, C. Stroh, and R. C. Witt, The two-dimensional hydrogen atom with a logarithmic potential energy function, Am. J. Phys. **58**, 1183 (1990).

[30] F. Gesztesy and L. Pittner, Electrons in logarithmic potentials. I. Solution of the Schrödinger equation, J. Phys. A **11**, 679 (1978).

[31] A. V. Turbiner and J. C. del Valle, *Quantum Anharmonic Oscillator* (World Scientific, Singapore, 2023).

[32] E. Mostaani, M. Szyniszewski, C. H. Price, R. Maezono, M. Danovich, R. J. Hunt, N. D. Drummond, and V. I. Fal'ko, Diffusion quantum monte carlo study of excitonic complexes in two-dimensional transition-metal dichalcogenides, Phys. Rev. B **96**, 075431 (2017).

[33] P. O. Löwdin, Eigenvalue problem in a linearly dependent basis and the super-secular-equation, Int. J. Quantum Chem. **1**, 811 (1967).

[34] A. V. Turbiner and M. A. Escobar-Ruiz, Two charges on a plane in a magnetic field: Hidden algebra, (particular) integrability, polynomial eigenfunctions, J. Phys. A **46**, 295204 (2013).

[35] H. Herold, H. Ruder, and G. Wunner, The two-body problem in the presence of a homogeneous magnetic field, J. Phys. B **14**, 751 (1981).

[36] R. Y. Kezerashvili and A. Spiridonova, Magnetoexcitons in transition metal dichalcogenides monolayers, bilayers, and Van der Waals heterostructures, Phys. Rev. Res. **3**, 033078 (2021).

[37] A. V. Stier, N. P. Wilson, K. A. Velizhanin, J. Kono, X. Xu, and S. A. Crooker, Magnetooptics of exciton Rydberg states in a monolayer semiconductor, Phys. Rev. Lett. **120**, 057405 (2018).

[38] J. C. del Valle and A. V. Turbiner, Radial anharmonic oscillator: Perturbation theory, new semiclassical expansion, approximating eigenfunctions. I. Generalities, cubic anharmonicity case, Int. J. Mod. Phys. A **34**, 1950143 (2019).

[39] A. M. Escobar-Ruiz, H. Olivares-Pilón, N. Aquino, and S. A. Cruz, Helium-like ions in D-dimensions: Analyticity and generalized ground state Majorana solutions, J. Phys. B **54**, 235002 (2022).

[40] A. V. Turbiner, W. Miller, and M. A. Escobar-Ruiz, Three-body problem in D-dimensional space: Ground state, (quasi)-exact-solvability, J. Math. Phys. **59**, 022108 (2018).

[41] D. Van Tuan, M. Yang, and H. Dery, Coulomb interaction in monolayer transition-metal dichalcogenides, Phys. Rev. B **98**, 125308 (2018).

[42] C. Fey, P. Schmelcher, A. Imamoglu, and R. Schmidt, Theory of exciton-electron scattering in atomically thin semiconductors, Phys. Rev. B **101**, 195417 (2020).

[43] A. V. Turbiner, J. C. Lopez Vieyra, J. C. del Valle, and D. J. Nader, Ultra-compact accurate wave functions for He-like and Li-like iso-electronic sequences and variational calculus: I. Ground state, Int. J. Quantum Chem. **121**, e26586 (2021).

[44] M. Z. Mayers, T. C. Berkelbach, M. S. Hybertsen, and D. R. Reichman, Binding energies and spatial structures of small carrier complexes in monolayer transition-metal dichalcogenides via diffusion Monte Carlo, Phys. Rev. B **92**, 161404(R) (2015).

[45] M. Szyniszewski, E. Mostaani, N. D. Drummond, and V. I. Fal'ko, Binding energies of trions and biexcitons in two-dimensional semiconductors from diffusion quantum monte carlo calculations, Phys. Rev. B **95**, 081301(R) (2017).